The Miller function, a sensitivity test for equations of state and theoretical vapor pressure data

S. Velasco [a], M.J. Santos [a], J.A. White [a,b,∗]

[a] Departamento de Física Aplicada, Universidad de Salamanca, 37008 Salamanca, Spain
[b] IUFFyM, Universidad de Salamanca, 37008 Salamanca, Spain

ABSTRACT

For non-quantum fluids, the Miller function, $h(T) = T \ln(p/p_c)/(T − T_c)$, with T_c and p_c the temperature and pressure at the critical point, presents a minimum in the liquid-vapor coexistence curve. By analyzing values from a NIST program for 105 fluids, we find that the temperature, T_M, of this minimum is closely correlated with the normal boiling temperature, T_b, and with the critical temperature of the fluid. We also demonstrate that the value of the minimum, $h_M = h(T_M)$, is well correlated with the acentric factor. We show that the Miller function can be used as a powerful tool for checking vapor pressure values obtained from equations of state or from vapor pressure equations, especially near the critical point.

© 2012 Elsevier Ltd. All rights reserved.

1. Introduction

Most of the proposed vapor pressure equations use the temperature T_c and the pressure p_c of the critical point as reducing values and provide the natural logarithm of the reduced vapor pressure, $p_r = p/p_c$, as a function of the reduced temperature, $T_r = T/T_c$,

$$\ln p_r = f(T_r), \tag{1}$$

where the function $f(T_r)$ contains, in general, several fluid dependent coefficients. For all fluids $f(T_r)$ is a negative function ($f(T_r) \leqslant 0$) that monotonically increases ($f'(T_r) > 0$) from the reduced temperature at the triple point to the value $f(1) = 0$ at the critical point. Besides the triple and critical points, the normal boiling point and the acentric point are other characteristic points on the reduced vapor pressure curve (aside from a few fluids with $T_{tp} > T_b$). No other characteristic points have been widely considered in the representation of $\ln p_r$ versus T_r.

Srinivasan et al. [1–4] and other papers describing their work [5–7] observed that the products of some liquid-vapor saturation properties exhibit peaks along the vapor pressure curves. These authors showed that these points, which define new characteristic properties of each fluid, exhibit close correlations with the critical properties, and that some of them are well correlated with the Pitzer acentric factor. These points have been used to optimize the coefficients in cubic equations of state [8], and to predict the properties of new low global warming potential refrigerants [9]. More

recently, Velasco et al. [10] analyzed the behavior of the Waring, $\psi(T) = −d \ln p/d(1/T)$, and Riedel, $\alpha(T) = d \ln p/d \ln T$, functions along the liquid–vapor coexistence curve for 105 fluids reported by the NIST program RefProp 9.0 [11]. They found that for most fluids $\psi(T)$ and $\alpha(T)$ present a minimum whose temperatures are also linearly correlated with the critical temperature T_c. Furthermore, by using reduced coordinates, they also showed that the minima are well correlated with the acentric factor. These correlations were used for testing some well-known vapor pressure equations in the Pitzer corresponding states scheme.

In this work we propose the Miller function, $h(T_r) = T_r \ln p_r/(T_r − 1)$ as an alternative to equation (1) for analyzing the behavior of the vapor pressure curve. This analysis is performed for vapor pressure values of 105 pure fluids reported by the NIST program RefProp 9.0 [11]. We show that, except for quantum fluids, the Miller function presents a minimum at a given reduced temperature, the reduced Miller temperature, T_{Mr}. We show that $T_M = T_{Mr}T_c$ is well correlated with both the normal boiling, T_b, and critical, T_c, temperatures. We also show that the minimum value of the Miller function, $h_M = h(T_{Mr})$, is correlated with the Pitzer acentric factor. Furthermore, near the critical point, the first derivative of $h(T_r)$ w.r.t. T_r presents the same divergence as the second derivative of the reduced vapor pressure. This behavior provides a powerful tool for checking vapor pressure data obtained from equations of state or from vapor pressure equations.

2. The Miller function

The simplest vapor pressure equation of type (1) is the so-called Clausius–Clapeyron (CC) equation

∗ Corresponding author at: Departamento de Física Aplicada, Universidad de Salamanca, 37008 Salamanca, Spain. Tel.: +34 923294436; fax: +34 923294584.
E-mail address: white@usal.es (J.A. White).

$$\ln p_r = A\left(1 - \frac{1}{T_r}\right) = A\frac{(T_r - 1)}{T_r}, \tag{2}$$

where A is a fluid characteristic coefficient. Equation (2) suggests one consideration of the dimensionless saturation function

$$h(T_r) \equiv \frac{T_r \ln p_r}{T_r - 1}, \tag{3}$$

as an alternative to equation (1) for analyzing the temperature dependence of the saturated pressure of a fluid along the liquid–vapor coexistence curve. Indeed, in terms of $h(T_r)$, the CC equation (2) can be rewritten in the form

$$h^{CC}(T_r) = A. \tag{4}$$

Therefore $h(T_r)$ provides a simple way to appreciate the deviation of the behavior of the vapor pressure of a given fluid with respect to the one prescribed by the Clausius–Clapeyron equation.

The calculation of $h(T_r)$ for selected characteristic points on the vapor pressure curve is direct:

1. By applying equation (3) at the reduced normal boiling temperature, $T_{br} = T_b/T_c$, the following value is derived

$$h_b \equiv h(T_{br}) = \frac{T_{br}}{T_{br} - 1} \ln \frac{101.325}{p_c}, \tag{5}$$

where p_c must be expressed in kPa. The parameter h_b was first introduced by Miller in 1963 [12], and it is known as the Miller parameter. This parameter has been used as a correlating quantity in some vapor pressure equations [13–19]. For this reason, we refer to the saturation function $h(T_r)$ defined by equation (3) as the Miller function.

2. From the definition of the Pitzer acentric factor [20,21],

$$\omega = -1.0 - \log_{10} p_r \quad \text{at } T_r = 0.7, \tag{6}$$

and using equation (3) one obtains

$$h_\omega \equiv h(0.7) = \frac{7 \ln 10}{3}(1 + \omega), \tag{7}$$

for the value of $h(T_r)$ at the acentric point temperature $T_r = 0.7$.

3. At the critical point equation (3) leads to an indetermination of 0/0 type. Then, by applying l'Hôpital's rule one has

$$h_c \equiv h(1) = \left(\frac{d \ln p_r}{dT_r}\right)_{T_r=1} = \left(\frac{dp_r}{dT_r}\right)_{T_r=1} = \alpha_c, \tag{8}$$

i.e, the value of $h(T_r)$ at the critical point $T_r = 1$ coincides with the Riedel factor α_c, the slope of the reduced vapor pressure at the critical point [22].

Figure 1 shows the variation of $h(T_r)$ with T_r for methane and nitrogen from the vapor pressure values reported by RefProp 9.0 [11]. This plot shows that the function $h(T_r)$ presents a minimum at a fluid dependent reduced temperature T_{Mr}. We shall refer to the minimum of the function $h(T_r)$ as the Miller point. The fact that $h(T_r)$ goes through a minimum at T_{Mr} is analytically expressed by the relation

$$h'(T_{Mr}) \equiv \left(\frac{dh(T_r)}{dT_r}\right)_{T_r=T_{Mr}}$$
$$= -\frac{\ln p_{Mr}}{(T_{Mr} - 1)^2} + \frac{T_{Mr}}{T_{Mr} - 1}\left(\frac{d \ln p_r}{dT_r}\right)_{T_r=T_{Mr}} = 0, \tag{9}$$

where $p_{Mr} = p_r(T_{Mr})$. From equations (3) and (9) one obtains

$$\left(\frac{d \ln p_r}{dT_r}\right)_{T_r=T_{Mr}} = \frac{h_M}{T_{Mr}^2}, \tag{10}$$

where $h_M = h(T_{Mr})$. Equation (10) shows that the slope of equation (1) at the Miller point can be obtained from the values T_{Mr} and h_M of
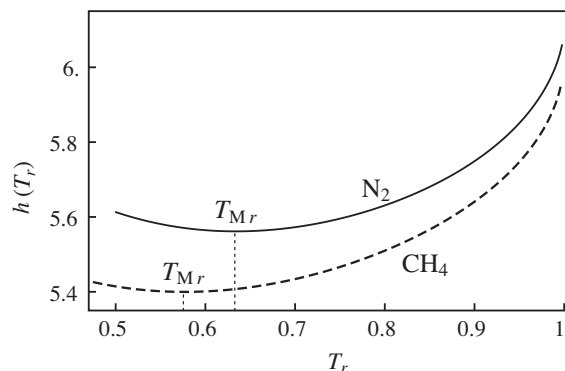

FIGURE 1. The Miller function $h(T_r)$ vs. the reduced temperature T_r for nitrogen (solid line) and methane (dashed line), indicating the positions of the minima, i.e., the reduced Miller temperatures T_{Mr}.

this point. This property enhances the importance of the Miller point as a reference point on the vapor pressure curve.

We have analyzed the function $h(T_r)$ with the use of the vapor pressure data of the 105 substances reported in RefProp 9.0, and listed the analysis in table S1 of the supplementary data. The Miller function $h(T_r)$ presents a minimum at a different reduced temperature T_{Mr} for all considered fluids except the quantum fluids (^{4}He, n-H$_2$, p-H$_2$, o-H$_2$, D$_2$ and Ne), ethanol, and propyne. We note that the lack of a minimum in the last two fluids could be due to the equations of state used in RefProp 9.0 (reference [23] for ethanol and reference [24] for propyne). We refer to $T_M = T_{Mr}T_c$ as the Miller temperature. We find that the Miller temperature T_M can be represented by the following quadratic relationship with the normal boiling temperature T_b,

$$T_M/\text{K} = -59.168 + 1.669(T_b/\text{K}) + 0.00096(T_b^2/\text{K}^2) \tag{11}$$

with a coefficient of determination $R^2 = 0.9876$. Figure 2(a) shows a plot of T_M vs. T_b. The symbols are data obtained from RefProp 9.0 [11] and reported in table S1 of the supplementary data, and the solid line corresponds to the correlation given by equation (11). Figure 2(b) shows the percent relative deviation ($10^2\Delta_r$) of T_M between tabulated values and values obtained using the correlation (11). The average absolute relative deviation (AARD) for all fluids is 3.6%. The maximum absolute relative deviation (MARD) is obtained for fluorine with a value of 22.7%.

We also find that the Miller temperature T_M presents the following linear relationship with the critical temperature T_c,

$$T_M/\text{K} = -35.204 + 0.84760(T_c/\text{K}). \tag{12}$$

with a coefficient of determination $R^2 = 0.9800$. Figure 3(a) shows a plot of T_M vs. T_c. Symbols correspond to RefProp 9.0 [11] data listed in table S1 of the supplementary data and the solid line corresponds to the correlation given by equation (12). Figure 3(b) shows the percent relative deviation of T_M between tabulated values and values obtained using the correlation (12). The AARD for all fluids is 4.5%. The MARD is obtained for xenon with a value of 22.3%.

We have also analyzed the values of the Miller function at the minimum, h_M, obtained for the fluids considered in the present work and reported in table S1 of the supplementary data. We find a linear correlation between h_M and the acentric factor ω given by

$$h_M = 5.39536 + 5.15675\,\omega, \tag{13}$$

with a coefficient of determination $R^2 = 0.9980$. Figure 4(a) shows a plot of h_M vs. ω. Symbols correspond to the RefProp 9.0 [11] values presented in table S1 of the supplementary data and the solid line corresponds to the correlation given by equation (13). Figure 4(b) shows the percent relative deviation ($10^2\Delta_r$) of h_M between
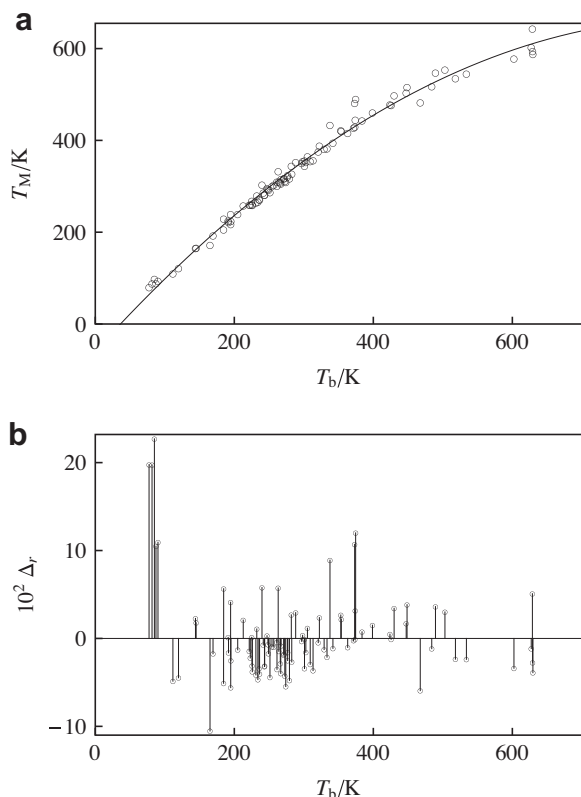
FIGURE 2. (a) The Miller temperature, T_M, vs. the normal boiling temperature, T_b. The line represents equation (11). (b) Percent relative deviations from equation (11). The symbols are the values obtained from RefProp 9.0 [11] (See table S1 of the supplementary data).

FIGURE 3. (a) The Miller temperature, T_M vs. the critical temperature, T_c. The line represents equation (12). (b) Percent relative deviations from equation (12). The symbols are the values obtained from RefProp 9.0 [11] (See table S1 of the supplementary data).

tabulated values and values obtained using the correlation (13). The AARD for all fluids is 0.39%. The MARD is obtained for MD3M with a value of 2.6%.

3. The Miller function for the Ambrose–Walton vapor pressure equation

Most of the vapor-pressure equations of type (1) proposed in the literature are expressed as a power series of ω,

$$\ln p_r = \sum_{k=0}^{n} \omega^k \phi_k(T_r), \qquad (14)$$

where $\phi_k(1) = 0$, and the functions $\phi_k(T_r)$ usually have the same analytical form for different values of k but include different adjustable parameters. Among these equations, it is widely recognized that the Ambrose–Walton (AW) equation [25], for which $n = 2$ and the functions $\phi_k(T_r)$ have the form of a Wagner vapor pressure equation

$$\phi_k(T_r) = \frac{1}{T_r}\Big[A_k(1-T_r) + B_k(1-T_r)^{1.5} + C_k(1-T_r)^{2.5} + D_k(1-T_r)^5\Big], \qquad (15)$$

correlates vapor pressure experimental data of pure fluids with fairly good accuracy from the triple to the critical point. The Miller function corresponding to the AW equation is given by

$$h^{AW}(T_r) = -\sum_{k=0}^{2} \omega^k\Big[A_k + B_k(1-T_r)^{0.5} + C_k(1-T_r)^{1.5} + D_k(1-T_r)^4\Big]. \qquad (16)$$

From this equation one can obtain the values of the Miller function at some characteristic points as functions of the acentric factor ω,
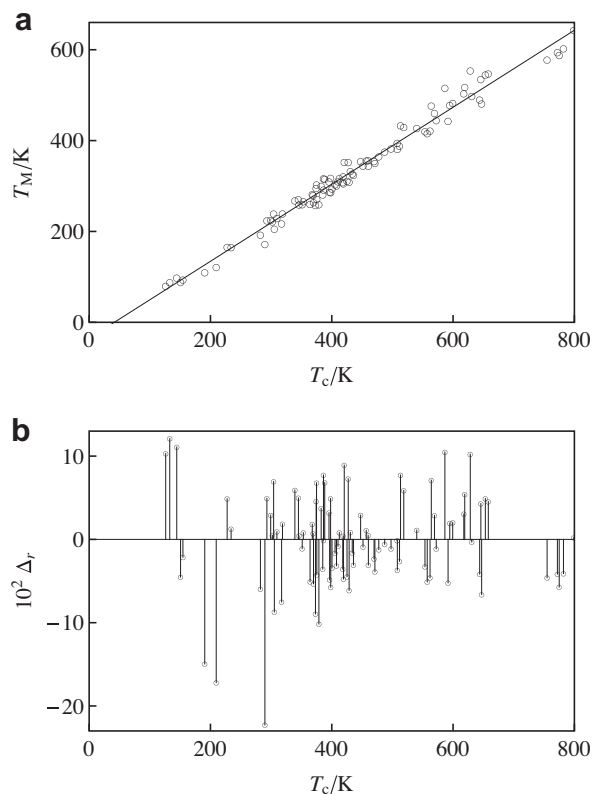
$$h_b^{AW} = -\sum_{k=0}^{2} \omega^k\Big[A_k + B_k(1-T_{br})^{0.5} + C_k(1-T_{br})^{1.5} + D_k(1-T_{br})^4\Big], \qquad (17)$$

$$h_\omega^{AW} = -\sum_{k=0}^{2} \omega^k\Big[A_k + 0.3^{0.5}B_k + 0.3^{1.5}C_k + 0.3^4 D_k\Big], \qquad (18)$$

and

$$h_c^{AW} = -\sum_{k=0}^{2} \omega^k A_k. \qquad (19)$$

As a direct application, comparison between Eqs. (7) and (18) gives absolute relative deviations less than 0.0001%. This is a consequence of the self-consistency of the AW equation to reobtain the acentric factor value used as an input [26].

On the other hand, the derivative of equation (16) w.r.t. T_r yields

$$h'^{AW}(T_r) = \sum_{k=0}^{2} \omega^k\Big[\frac{B_k}{2}(1-T_r)^{-0.5} + \frac{3C_k}{2}(1-T_r)^{0.5} + 4D_k(1-T_r)^3\Big]. \qquad (20)$$

Using this equation, equation (9) leads to

$$\sum_{k=0}^{2} \omega^k\Big[B_k + 3C_k(1-T_{Mr}^{AW}) + 8D_k(1-T_{Mr}^{AW})^{3.5}\Big] = 0, \qquad (21)$$

which allows us to obtain numerically the reduced Miller temperature, T_{Mr}^{AW}, as a function of the acentric factor ω for the AW equation. Finally, substitution of T_{Mr}^{AW} in equation (16) allows one to obtain h_{Mr}^{AW} as a function of ω for the AW equation.

Figure 5(a) shows a plot of T_{Mr} vs. ω. Symbols correspond to tabulated data reported in table S1 of the supplementary data.
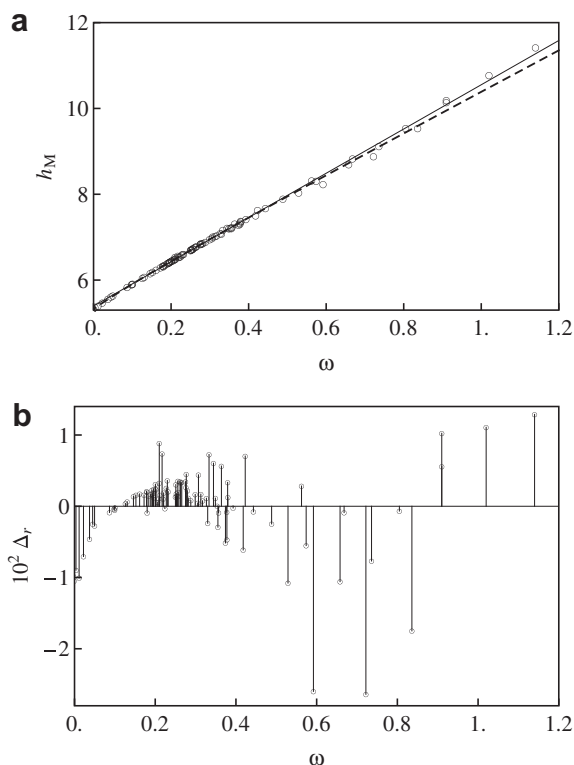
FIGURE 4. (a) The value of the Miller function at its minimum, h_M, vs. the acentric factor, ω. The symbols are the values obtained from RefProp 9.0 [11] (See table S1 of the supplementary data). The solid line represents the correlation given by equation (13). The dashed line is the minimum value of the Miller function obtained from the AW equation (see text). (b) Percent relative deviations from equation (13).

FIGURE 5. (a) The reduced Miller temperature, T_{Mr}, vs. the acentric factor, ω. The symbols are the values obtained from RefProp 9.0 [11] (See table S1 of the supplementary data). The solid line represents the AW result, obtained from equation (21). (b) Percent relative deviations from the AW result.

Figure 5(a) shows that for low ω values T_{Mr} increases as ω increases. The variation of T_{Mr}^{AW} versus ω obtained from the AW equation is plotted by a solid line in figure 5(a). The AW equation gives a value of $\omega = -0.118$ below which T_{Mr}^{AW} becomes negative. This limit occurs where quantum fluids do not have a minimum for the Miller function. The AW equation provides T_{Mr}^{AW} values increasing with ω. This behavior agrees with the tabulated data for low ω. Figure 5(b) shows the percent relative deviation of T_{Mr} between tabulated values and values obtained using the AW equation. An AARD of 2.4% between AW values and tabulated data for T_{Mr} is obtained. A MARD of 11.5% is obtained for methyl stearate. Large deviations are also obtained for the other fluids with $\omega > 0.9$, namely, methyl linolenate, methyl oleate, and methyl palmitate.

The variation of h_{Mr}^{AW} versus ω obtained from the AW equation is plotted by a dashed line in figure 4(a). One can see that h_{Mr}^{AW} increases with ω in a practically linear way very close to the correlating equation (13) for low ω. An AARD of 0.31% between AW values and tabulated data for h_{Mr} is obtained. In this case we obtain a MARD of 3.1% for methyl linolenate. As in figure 5(a), in figure 4(a) one can observe that the four fluids with $\omega > 0.9$ show the larger deviations with respect to the AW result.

Figure 6(a) shows $\ln p_r$ vs. T_r for water from the vapor pressure data reported by the NIST program. The variation of $\ln p_r$ versus T_r obtained from the AW equation is also plotted by a dashed line in figure 6(a). One can see that, except near the triple point, the AW equation reproduces the NIST values with rather good accuracy. However, when one plots $h(T_r)$ vs. T_r, as it is shown in figure 6(b), one can appreciate the discrepancies between values obtained from the AW equation and those obtained from NIST calculations. These discrepancies come from the deviation of T_{Mr}^{AW} from the T_{Mr} data obtained from the NIST program. Therefore, the Miller function $h(T_r)$ seems to be a more sensitive function than $\ln p_r$ to
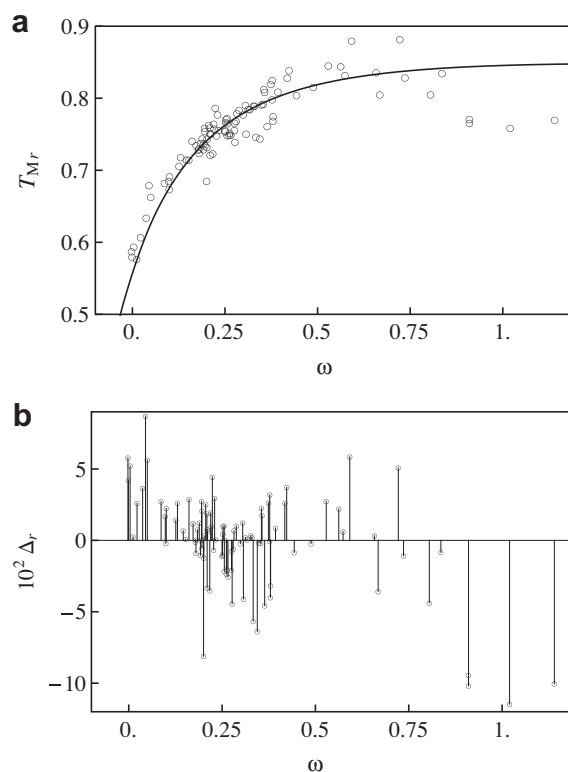
compare vapor pressure data coming from smoothed experimental and correlating equations.

4. The Miller function near the critical point

Figure 1 also shows an interesting characteristic of the function $h(T_r)$: the slope is *positive* near the the critical point. However, we have found that the slope of the Miller function of some fluids reported by the NIST program is *negative* near the critical point. For example, this is the case for hexane and ethanol, for which the Miller function is plotted vs. T_r in figures 7 and 8 from the vapor pressure data reported in the NIST program using the equations of state of references [28] (hexane) and [23] (ethanol). Furthermore, for some of these fluids (e.g., fluorine) $h(T_r)$ becomes negative very close to the critical point (note that NIST results for fluorine are obtained from the equation of state of reference [29]). But, this is not possible because h_c must always be positive. In order to verify the validity of an equation of state one needs to analyze the behavior of $h(T_r)$ near the critical point.

Near the critical point, $h(T_r)$ must be consistent with extended thermodynamic scaling for the vapor pressure around this point. In particular, as one approaches the critical point, renormalization group theory establishes that the second derivative of the vapor pressure with respect to the temperature diverges following the scaling law [30]

$$\frac{d^2 p_r}{dT_r^2} \approx B(1 - T_r)^{-\alpha}, \tag{22}$$

where α is the critical exponent for the heat capacity at constant volume and B is a fluid dependent positive coefficient. Taking into account the relation
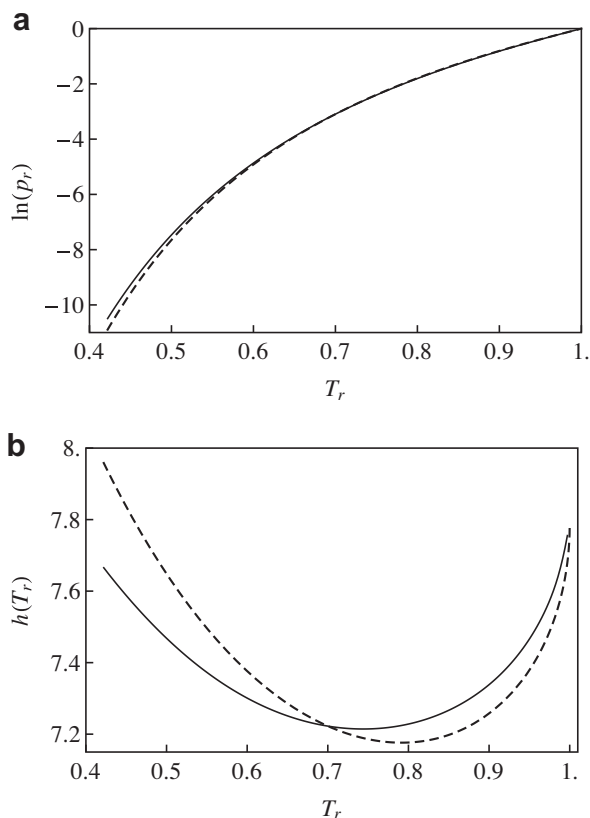
a

b

FIGURE 6. Comparison of the results of RefProp 9.0 [11] (solid line) and the AW equation (dashed line) for water. (a) $\ln p_r$ vs. T_r. (b) $h(T_r)$ vs. T_r.
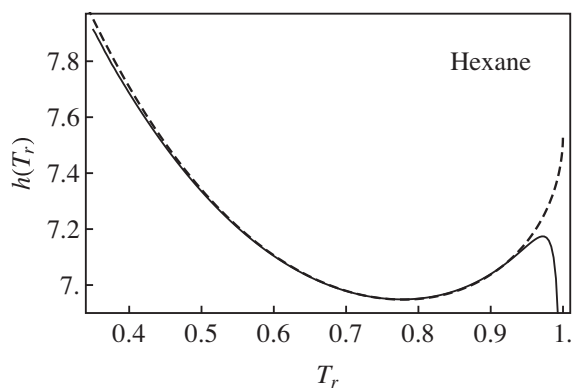

FIGURE 7. The Miller function $h(T_r)$ vs. T_r for hexane. The solid line is the result obtained from RefProp 9.0 [11]. The dashed line is the result obtained from the AW equation.

$$\frac{d^2 \ln p_r}{dT_r^2} = -\frac{1}{p_r^2}\left(\frac{dp_r}{dT_r}\right)^2 + \frac{1}{p_r}\frac{d^2 p_r}{dT_r^2}, \tag{23}$$

since p_r and dp_r/dT_r remain finite at the critical point, scaling law, equation (22), implies that

$$\frac{d^2 \ln p_r}{dT_r^2} \approx B(1 - T_r)^{-\alpha}, \tag{24}$$

when T_r approaches 1 (critical point). Taking into account the values at the critical point, $\ln p_r = 0$ at $T_r = 1$, integrating equation (24) twice yields
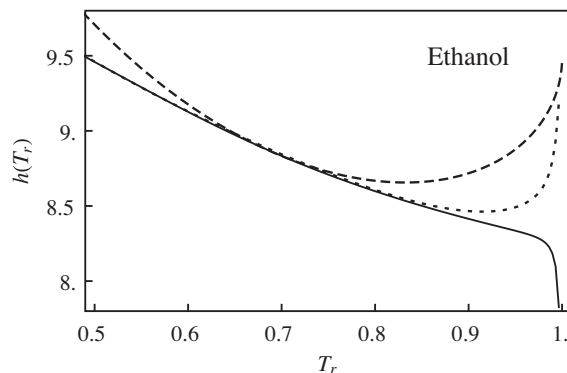

FIGURE 8. The Miller function $h(T_r)$ vs. T_r for ethanol. The solid line is the result obtained from RefProp 9.0 [11]. The dashed line is the result obtained from the AW equation. The dotted line is obtained from RefProp using an improved equation of state [27].

$$\ln p_r = A_1(1 - T_r) + A_2(1 - T_r)^{2-\alpha} + \cdots \tag{25}$$

near the critical point, where $A_1 = -\alpha_c = -h_c$, according with equation (8), and $A_2 = B/(1-\alpha)(2-\alpha)$. Using expansion (25), equation (3) leads to

$$h(T_r) \approx -\left[A_1 + A_2(1 - T_r)^{1-\alpha} + \cdots\right] \tag{26}$$

near the critical point. The derivative of equation (26) w.r.t. T_r, leads to

$$h'(T_r) \approx (1 - \alpha)A_2(1 - T_r)^{-\alpha} = \frac{B}{2-\alpha}(1 - T_r)^{-\alpha} \tag{27}$$

near the critical point. Equation (27) shows that if $d^2 p_r/dT_r^2$ verifies the scaling law given by equation (22), $h'(T_r)$ also verifies the same scaling law.

Equation (20) shows that the AW equation satisfies scaling law (27) with an effective critical exponent $\alpha = 0.5$. The AW equation for hexane and NIST calculations are in an excellent agreement (not plotted). However, the Miller function (16) for the AW equation (plotted by a dashed line in figure 7 shows an evident discrepancy with NIST values (solid line) in the region of $T_r \geqslant 0.95$. A similar behavior is observed for ethanol which is plotted by a solid line in figure 8 (note the lack of a minimum for $T_r < 1$). In this case we also plot NIST results with an improved equation of state [27] (dotted line) and the AW Miller function (dashed line) noting that in these two cases the Miller function has a minimum and shows the expected behavior near the critical point. The equation of state in Reference [27] will be the new equation used in future versions of RefProp [31].

5. Summary

To summarize, we propose the Miller function, $h(T_r) = T_r \ln p_r/(T_r - 1)$, as an alternative to the natural logarithm of the reduced vapor pressure, $\ln p_r$, to analyze the temperature dependence of the vapor pressure along the liquid–vapor coexistence line. By using vapor pressure data of 105 fluids reported in RefProp 9.0, we have shown that, except for the quantum fluids and two other fluids, the Miller function presents a minimum at a fluid dependent reduced temperature T_{Mr}. Two interesting empirical relations have been derived between the temperature, $T_M = T_{Mr}T_c$, of the minimum and the normal boiling temperature, T_b, and the critical temperature, T_c. Furthermore, we have shown that the value of the minimum, h_M, presents a linear correlation with the Pitzer acentric factor, ω. We have analyzed the Miller function for the Ambrose–Walton vapor pressure equation. This equation

allows one to obtain T_{Mr} and h_M as functions of ω. These functions present fairly good agreement with the values obtained from Ref-Prop 9.0. We show that the Miller function is more sensitive than the vapor pressure equation for checking vapor pressure data. Finally, by using the renormalization group divergence for the second derivative of the vapor pressure, we show that the Miller function must present the same type of divergence. This behavior is checked for the NIST fluids, finding that not all of them present such divergence.

Acknowledgements

Appendix A. Supplementary data

Supplementary data (Table S1) associated with this article can be found, in the online version, at http://dx.doi.org/10.1016/j.jct.2012.10.019.

References

[1] S. Khan, K. Srinivasan, High Temp. High Press 26 (1994) 427–438.
[2] S. Khan, K. Srinivasan, High Temp. High Press. 26 (1994) 519–530.
[3] S. Khan, K. Srinivasan, J. Phys. D: Appl. Phys 29 (1996) 3079–3088.
[4] K. Srinivasan, Z. Phys. Chem. 216 (2002) 1379–1387.
[5] F.L. Román, J.A. White, S. Velasco, A. Mulero, J. Chem. Phys. 123 (2005) 124512-1–124512-6.
[6] S. Velasco, F.L. Román, J.A. White, A. Mulero, Appl. Phys. Lett. 90 (2007) 141905-1–141905-3.
[7] S. Velasco, F.L. Román, J.A. White, J. Chem. Eng. Data 55 (2010) 4244–4247.
[8] J. Tian, H. Jiang, Y. Xu, Mod. Phys. Lett. B 23 (2009) 3091–3096.
[9] K. Srinivasan, K.C. Ng, S. Velasco, J.A. White, J. Chem. Thermodyn. 44 (2012) 97–101.
[10] S. Velasco, J. White, K. Srinivasan, P. Dutta, Ind. Eng. Chem. Res. 51 (2012) 3197–3202.
[11] E.W. Lemmon, M.L. Huber, M.O. McLinden, NIST Standard Reference Database 23: Reference fluid thermodynamic and transport properties-REFPROP, version 9.0, howpublishedNational Institute of Standards and Technology, Standard Reference Data Program, Gaithersburg, 2010.
[12] D.G. Miller, Ind. Eng. Chem. 2 (1963) 78–79.
[13] D.G. Miller, J. Phys. Chem. 69 (1965) 3209.
[14] M. Gomez-Nieto, G. Thodos, Ind. Eng. Chem. Fundam. 16 (1977) 254–259.
[15] M. Gomez-Nieto, G. Thodos, Can. J. Chem. Eng. 55 (1977) 445–449.
[16] M. Gomez-Nieto, G. Thodos, Ind. Eng. Chem. Fundam. 17 (1978) 45–51.
[17] A. Vetere, Fluid Phase Equilib. 62 (1991) 1–10.
[18] A. Vetere, Ind. Eng. Chem. Res. 30 (1991) 2487–2492.
[19] A. Vetere, Fluid Phase Equilib. 240 (2006) 155–160.
[20] K.S. Pitzer, J. Am. Chem. Soc. 77 (1955) 107–113.
[21] K.S. Pitzer, D.Z. Lippmann, R.F. Curl, C.M. Huggins, D.E. Petersen, J. Am. Chem. Soc. 77 (1955) 3433–3440.
[22] L. Riedel, Chem. Eng. Tech. 26 (1954) 83–89.
[23] H. Dillon, S. Penoncello, Int. J. Thermophys. 25 (2004) 321–335.
[24] A. Polt, B. Platzer, G. Maurer, Chem. Tech. (Leipzig) 44 (1992) 216–224.
[25] D. Ambrose, J. Walton, Pure Appl. Chem. 61 (1989) 1395–1403.
[26] S. Velasco, J.A. White, J. Chem. Eng. Data 56 (2011) 1163–1166.
[27] J.A. Schroeder, titleA New Fundamental Equation for Ethanol, Master's thesis, University of Idaho, 2011.
[28] R. Span, W. Wagner, Int. J. Thermophys. 24 (2003) 41–109.
[29] K. de Reuck, International Thermodynamic Tables of the Fluid State-11 Fluorine, Pergamon Press, Oxford, 1990.
[30] H.E. Stanley, Introduction to Phase Transitions and Critical Phenomena, Oxford University Press, New York, 1971.
[31] E.W. Lemmon, Private Communication (2012).

JCT 12-407